Thermal Desktop Modeling of the 2016 CRYOTE-2 Tank Chilldown and Fill Testing

Erin Tesny[a] and Jason Hartwig[a]

[a]NASA Glenn Research Center, Fluids and Cryogenics Branch, Cleveland, OH, 44135

Abstract

The storing and transfer of cryogenic propellants is an enabling technology for NASA and industry as civilization moves to expand future missions into low Earth orbit and beyond. Several ground propellant transfer tests have been conducted in past decades examining various tank chilldown and fill methods. Creating accurate models using these historical datasets is a vital step toward developing appropriate modeling tools to form pre-test predictions for subsequent ground and flight propellant transfers. This paper presents model validation of Thermal Desktop using data from the 2016 CRYOTE-2 liquid nitrogen transfer experiments whose purpose was to demonstrate the chill and fill process in a spherical receiver tank. Tank pressure, fill level, and wall temperature were all modeled and compared with 8 test cases using two modeling methods, Mass Controlled, and Pressure Controlled. This test series is the hardest Thermal Desktop tank chill and fill validation case to-date, yet the model was able to accurately predict each of these metrics for the 2016 tests within 28%, 10%, 20% respectively, for pressure, fill level, and wall temperature using the Mass Controlled model, and 29%, 79%, and 12%, respectively for the Pressure Controlled model.

Keywords: no-vent fill, Thermal Desktop, chilldown, condensation, liquid nitrogen

1.0 Introduction

The storing and transfer of cryogenic propellants is an enabling technology for NASA and industry as civilization moves to expand future missions into Low Earth Orbit (LEO) and beyond. The transfer of cryogenic propellants is of particular interest because it has never been successfully demonstrated in microgravity to-date. An in-space propellant transfer is divided into various stages, including (1) pressurization of the supply tank, (2) propellant management devices to extract single-phase liquid, (3) transfer line chilldown, (4) receiver tank chilldown, and (5) receiver tank fill. This paper focuses on modeling stages 4 and 5.

While somewhat inefficient, the cryogenic transfer process in 1-g is trivial; the receiver tank is vented throughout the transfer, and the boil-off vapor produced during chilldown is vented through the top of the tank while the liquid accumulates to the desired final fill level. In microgravity, where the fluid is in an unsettled configuration however, propellant transfer is complicated by the unknown location of the liquid/vapor interface, complex heat transfer processes, and propensity to vent liquid. Due to the high cost of launching and storing propellant in space, venting liquid is to be avoided at all times.

Cryogenic propellants such as liquid oxygen (LO_2) are prone to boiling at low heat flux (relative to water), causing pressure rise rates that can disrupt the transfer process. Furthermore, complex two-phase flows can arise, which would complicate system modeling efforts, making the transfer process more unpredictable. At the time of writing this paper, no reduced gravity cryogenic chill and fill transfer experiments have been conducted. In lieu of experimentation in the space environment, ground tests have been conducted that still capture many of the operational issues and heat and mass transfer processes that arise during cryogenic propellant transfer. As a result, several chilldown and fill methods have been conceived and tested over the

past several decades to address the difficulties of transferring cryogens in reduced gravity environments.

The simplest method is to utilize a cryocooler heat exchanger to prechill the receiving tank, followed by a continuous no-vent fill (NVF). Spaceflight cryocoolers with high efficiency are still in development and require additional system mass, power, and complexity. Without cryocoolers, the cooling capacity of the propellant must be used to chill down the transfer hardware. However, this leads to loss of propellant; the liquid undergoes phase change and is vented overboard. Thus, is it necessary to remove as much thermal energy as possible to conserve propellant. A second candidate chill and fill method was first proposed by [1] and later explored analytically by [2, 3] deemed the charge/hold/vent (CHV) method. Here, a "charge" of liquid is introduced into the tank with the receiver tank vent valve closed. The liquid is then held for some time to allow complete phase change. The fluid and wall reach thermal equilibrium at a new lower temperature. Then the vapor is vented, and the process is repeated until the wall temperature reaches the "target temperature" [4] that is cold enough to allow a NVF. The CHV method alleviates the possibility of venting liquid but introduces complexity due to valve cycling, extended transfer duration, and the need to potentially gauge mass in the tank. A third proposed method is called the vented chill (VC)/NVF originally demonstrated in [5]. Here, the receiver tank vent valve remains open until the receiver tank reaches the target temperature, followed by a continuous NVF. The goal of VC/NVF is to expedite the transfer process through less valve cycling, however, care must be taken to ensure the injection method maximizes the evaporation rate between receiver tank ullage and incoming liquid as well as the boiling heat transfer between liquid and wall to prevent any liquid from being vented. The VC/NVF method is the focus of this paper. A fourth method that was recently devised at NASA Marshall Space

Flight Center (MSFC) was the thermodynamic vent system (TVS) assisted transfer. Here, the propellant transfer is conducted with the main vent valve closed; the injector has an embedded TVS heat exchanger where a small amount of liquid from the main injection line is routed through a Joule-Thomson device, expanded, cooled, and integrated with the injector to assist in subcooling the main injection line. Data analysis from [6] showed, however, that the benefit of the TVS was in chilling down the injector itself and allowing a stalled transfer to recommence due to a new condensation heat transfer path opening up between the cold injector and warm ullage. This TVS-assisted NVF still requires further testing to prove to be a viable concept.

This paper presents Thermal Desktop (TD) model development and validation against the CRYogenic Orbital Testbed Experiment-2 (CRYOTE-2) 2016 tests, a recent set of experiments conducted at NASA MSFC. In total 53 tests were performed, using three different liquid injection systems, over a wide range of thermodynamic conditions and flow rates. The focus of this paper is on model validation against a single particular spray device for 8 validation cases. The outline of the paper is as follows: First a background section is given to briefly discuss previous chill and fill testing and modeling. Next, the description of the CRYOTE-2 system, hardware, experiment, and instrumentation is presented. Then, a brief description of the Thermal Desktop model is given, along with test-specific assumptions, boundary conditions, initial conditions, and final conditions. Finally, Thermal Desktop model results are compared with test data along with some discussion.

2.0 Background

1-g cryogenic transfer experiments have been conducted for decades. What follows is a brief summary of those tests; for a detailed history of cryogenic chill and fill testing and modeling, the reader is referred to [4]. Fester [7] performed NVF tests with Freon-113 on a

vertical cylinder using a bottom fill method. Chato et al. [8] and [9] then used a top spray nozzle injector on a cylindrical tank using liquid nitrogen (LN_2) and LH_2. [10] subsequently conducted NVF tests on the same tank using LH_2, but tested the performance of a top spray nozzle, upward pipe discharger, and bottom diffuser. The last was used to simulate low-g cases where the injector would be submerged. Chato [11] conducted NVFs on an aluminum sphere using LH_2 with a top spray nozzle and bottom jet. Chato and Sanabria [1] conducted CHV tests on the same tank. Moran and Nyland [12] investigated the performance of a spray bar using LN_2 on a vertical cylinder. Chato [13] tested a spray bar using LH_2. Wang and Wang [14], Wang et al. [15], and Kim et al. [16] conducted parametric NVF tests using multiple injectors. Flachbart et al. [17] conducted NVF tests on the thick-walled Multi-purpose Hydrogen Testbed using LH_2. Hartwig et al. [4] reported results of the CRYOTE-2 test program while [5] and [6] reported test results of the TVS-assisted injector test data analysis and the original rapid chill and fill tests, respectively.

Analysis performed in the current work falls under the Reduced Gravity Cryogenic Transfer (RGCT) project at NASA whose goals are (1) to investigate efficient cryogenic chilldown and transfer methods in a reduced gravity environment to enable future flight transfer systems, and (2) to develop and validate improved empirical, analytical, lumped capacitance, and computational fluid dynamics models for propellant transfer operations in terrestrial and reduced gravity environments. RGCT is producing direct-cryogenic data anchored propellant transfer models at multiple levels, including fundamental cryogenic boiling heat transfer and pressure drop correlations [18-20], a first-principles analytical model that predicts the failure of a NVF with 100% accuracy [21], various design tools for cryogenic tank chilldown and fill injection methods, including (TVS)-assisted injectors, development and validation of lumped capacitance codes Thermal Desktop and the Generalized Fluid System Simulation Program (GFSSP) for tank

chilldown and tank fill [22-24], CFD of tank chilldown using FLUENT [25]and CFD of the fluid dynamics inside a propellant tank subject to sloshing and non-inertial forces in reduced gravity [26]. Analysis in the current work is focused on validation of Thermal Desktop for the CRYOTE-2 tank chilldown and fill experiments. This test series represents the hardest validation case performed to-date. Relative to previous Thermal Desktop validation exercises against larger tanks with smaller temperature differences and longer transfer time scales, the chilldown and fill process for CRYOTE-2 transfers is relatively faster here, the injectors are the most complicated, and the temperature gradients between wall and fluid are the highest studied.

3.0 Experimental Description

As stated in [4], "CRYOTE was first envisioned by the United Launch Alliance and initial concepts were first reviewed in 2008 [27]. CRYOTE was designed to test a completely integrated cryogenic test bed for testing fuel storage and transfer in as close to a flight environment as possible. Subsystems of CRYOTE include multi-layer insulation (MLI) to reduce parasitic heat leak, a support skirt, a TVS for managing pressure in the tank through cooling/venting the fuel, a vapor cooled heat exchanger running through the skirt for maximizing the usefulness of the TVS, and a liquid level sensing system." This paper specifically focuses on the chill and fill tests that occurred in 2016, where the emphasis was on obtaining data for simple, higher performing injectors, as well as examining the effect of different thermodynamic parameters.

3.1 Hardware Description

The CRYOTE test series was conducted at NASA MSFC in the Exploration Systems Test Facility (ESTF). ESTF is a 6.10 m long, 2.74 m diameter multi-purpose vacuum chamber that has been used for numerous cryogenic fluid management experiments at the Marshall Space

Flight Center. The test set up consisted of a supply tank, receiver tank, transfer line, vent line, and various instrumentation inside a vacuum chamber shown in Figure 1. The Vibro-Acoustic Test Article (VATA) is the supply tank that feeds the CRYOTE receiver tank inside of the ESTF. During the CRYOTE tests, VATA is filled with LN2 initially at 77K and 1 atm and then pressurized to the desired supply tank pressure utilizing gaseous nitrogen (GN_2).

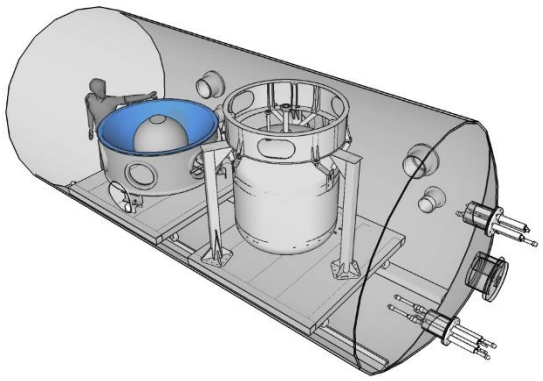

Figure 1 – System Diagram for the 2016 CRYOTE-2 Transfer Tests. From left to right: CRYOTE tank, VATA tank

The CRYOTE receiver tank will be the main focus of this study. The CRYOTE receiver tank shown in Figure 2 is a spherical 6-4 titanium (Ti) tank with an OD of 75.44 cm, 0.127 cm wall thickness, and an MAWP of 5.7 MPa (827) psi at cryogenic temperatures. The volume of CRYOTE at room temperature is 0.221 m^3 (7.82 ft^3) but is 0.216 m^3 at 77K (7.62 ft^3) due to metal contraction. The spherical portion of the tank weighs approximately 10.3 kg. The tank lid, on the other hand, is a thick cylindrical 304SS lid that weighs approximately 2.9 kg. These masses do not include the small masses of the injectors and connectors into the lid. An MLI skirt was placed around the receiver tank to reduce the heat load into the bottom of the tank.

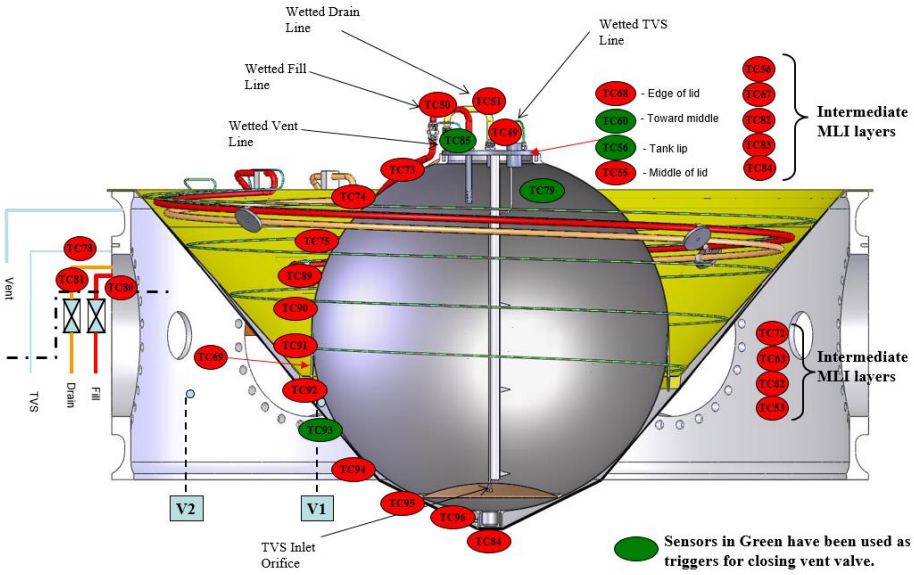

Figure 2 – 2016 CRYOTE 2 Thermocouple Locations

Three injectors were tested in total, but only one was tested for the 2016 tests. The spray pattern for this injector is shown in Figure 3. From [4], this injector used one BETE 0.33 cm (0.13 in), 170° TF8 spray nozzle facing upwards, one BETE 0.41 cm (0.16 in), 170° TF10 spray nozzle facing downwards, and a BETE 0.23 cm (0.09 in), 170° TF6 spray nozzle facing downwards. As shown, this injector appears to atomize the spray well. This injector has an overall coefficient of discharge of $C_D = 0.800$ with 32.5% of the flow going through TF8 on the left, 50% of the flow heading through TF10 in the center, and the remaining 17.5% of the flow heading through TF6 on the right [28] where coefficient of discharge is defined as:

$$C_D = \frac{\dot{m}}{A\sqrt{2\rho\Delta P}} \tag{1}$$

where ρ is the liquid density based on inlet temperature and pressure, A is the sum of the area of the injector holes, ΔP is the measured pressure drop between two points, and $\dot{m}$ is the flow rate determined from the following equation:

$$\dot{m} = \frac{dm_{LC}}{dt} - \dot{m}_{tap} \tag{2}$$

where m_{LC} is the mass measurement from the CRYOTE tank load cells and $\dot{m_{tap}}$ is the small gas flow rate out of a small vent tap that was open (not main vent valve), roughly 1/300 of the main liquid inlet flow rate. Note that these equations only apply during tank fill when single phase liquid is present.

Figure 3: Fluid Injector for the 2016 Tests

3.2 Instrumentation

The receiver tank, MLI skirt, and feed lines were fitted with various thermocouples and to measure the temperature inside and outside the tank as shown in Figure 2 and outlined in Table 1. Of particular interest are thermocouples TC73-TC96 which were placed on the outside of the tank wall in a vertical line which were used to estimate the temperature distribution as the tank fills. There were also three load cells placed beneath the tank to measure the change in mass as the tank fills. Pressure transducers were also placed in the fill line and inside the tank. Unfortunately, there were no flow meters on the pressurant gas line into VATA nor in the transfer line connecting VATA to CRYOTE, nor on the vent line, making it impossible to determine the amount of liquid entering into CRYOTE during transfer line chilldown and tank chilldown where two-phase flow was present. Regardless, analysis in the current work is focused on NVF, and by that point in transfer, the inlet state into the receiver tank is primarily single-

phase liquid, the receiver tank vent valve was closed, and the load cell data could be used directly to determine the mass flow rate into the tank.

From [4]: uncertainty in the sensors is as follows. The thermocouples had a margin of error of +/- 2 degrees K. Pressure transducers had a +/- 0.5% Best Fit Straight Line (BFSL) margin of error. Load cells and volumetric flow meters had an uncertainty < 2% full scale. The nominal record rate for all data was 1 Hz.

CRYOTE Sensors					
Thermocouple Location Description	**DAQ ID**	**Uncertainty**	**Thermocouple Location Description**	**DAQ ID**	**Uncertainty**
Wetted thru TVS tee at Lid ~ 39.5% fill level	TC49	+/- 2 degrees K	Transfer line TC, 47" from TC 86 (right before Valve Z)	TC87	+/- 2 degrees K
Wetted Fill at Lid	TC50	+/- 2 degrees K	Transfer line TC, 16" from TC 87 (right before tee with CRYOTE drain line)	TC88	+/- 2 degrees K
On skirt inside turn 1 from tank	TC52	+/- 2 degrees K	71.9% fill level, external to tank	TC89	+/- 2 degrees K
On skirt inside turn 4 from tank	TC54	+/- 2 degrees K	57.5% fill level, external to tank	TC90	+/- 2 degrees K
Close to center of lid	TC55	+/- 2 degrees K	42.5% fill level, external to tank	TC91	+/- 2 degrees K
CRYOTE tank lip (at lid but on main tank body)	TC56	+/- 2 degrees K	28.1% fill level, external to tank	TC92	+/- 2 degrees K
On skirt inside turn 2 from tank	TC57	+/- 2 degrees K	15.5% fill level, external to tank	TC93	+/- 2 degrees K
On skirt inside turn 5 from tank	TC58	+/- 2 degrees K	6.0% fill level, external to tank	TC94	+/- 2 degrees K
Tank Lid, half way between edge and center of lid	TC60	+/- 2 degrees K	0.7% fill level, external to tank	TC95	+/- 2 degrees K
TVS turn 5 from tank	TC61	+/- 2 degrees K	0.0% fill level, external to tank	TC96	+/- 2 degrees K
on skirt inside turn 3 from tank	TC64	+/- 2 degrees K			
TVS turn 3 from tank	TC65	+/- 2 degrees K			
TVS turn 4 from tank	TC66	+/- 2 degrees K	**Cryote Load Cells**	**DAQ ID**	
Edge of Tank Lid, thicker part	TC68	+/- 2 degrees K	Load Cell 4	SG004	unknown
TVS turn 2 from tank	TC70	+/- 2 degrees K	Load Cell 5	SG005	unknown
99.3% Fill level, external to tank	TC73	+/- 2 degrees K	Load Cell 6	SG006	unknown
94.0% fill level, external to tank	TC74	+/- 2 degrees K			
84.4% fill level, external to tank	TC75	+/- 2 degrees K	**Pressure Transducers**	**DAQ ID**	
CRYOTE Wetted 95% fill level	TC79	+/- 2 degrees K	Pressure upstream of Spray Head	AI50	+/- 0.5% BFSL
tank fill line at ESPA ring	TC80	+/- 2 degrees K	Pressure TVS Vent Line at HX	AI51	+/- 0.5% BFSL
Temp CRYOTE Spray	TC82	+/- 2 degrees K	Pressure CRYOTE2 ullage tap (dedicated)	AI52	+/- 0.5% BFSL
Temp TVS Vent at HX	TC83	+/- 2 degrees K	Pressure TVS Flowmeter	AI53	+/- 0.5% BFSL
Tank sump at base of cup (Very bottom of tank)	TC84	+/- 2 degrees K			
Wetted Vent at Lid	TC85	+/- 2 degrees K	**Flow Meters**	**DAQ ID**	
Transfer line TC, 60" from VATA TC36	TC86	+/- 2 degrees K	TVS Volumetric Flow Meter	FM-T362	unknown

Table 1: CRYOTE Sensor Names, Locations, and Units

3.3 Test Methodology

To properly transfer propellant into a warm tank, the CRYOTE tank wall must first be cooled to prevent the pressure front exceeded the maximum expected operating pressure (MEOP) during fill. The injector used in the 2016 CRYOTE-2 test was designed to rapidly remove heat from the wall during chilldown and then to subsequently cool the ullage during fill.

The chilldown was performed with the vent valve open, described earlier in Section 2.0 as the VC. The trigger point for the end of chilldown differed between the different tests but was most commonly an average wall temperature. Once this point was reached, the vent valve was then closed at the end of chilldown so that a NVF could be performed. More details on the test methodology are in [4].

4.0 Test Matrix and Operating Conditions

Tables 2 and 3 present the test matrix, along with initial conditions, boundary conditions, and final conditions. Since two-phase flow always existed during the initial stages of the transfer process due to transfer line chill down, the inlet state of the flow into CRYOTE is indeterminable with the sensors utilized in the experiment during this phase. Therefore, it is not possible to accurately model the initial chilldown portion of transfer due to two-phase flow. Therefore, direct comparison with the model is achievable only during the NVF portion of transfer.

Date	VATA Supply Pressure	Avg CRYOTE Inlet Pressure during NVF	TC50 Median during NVF	CRYOTE Tank Pressure at NVF Start	CRYOTE Ullage Temp at NVF Start	CRYOTE Mass Liquid at NVF Start	CRYOTE Mass Vapor at NVF Start	CRYOTE LL at NVF Start	CRYOTE Mass Avg Tank Temp at NVF Start
Test Name	kPa	kPa	K	kPa	K	kg	kg	% Fill	K
20160914	310.3	288.83	85.88	261.53	86.75	1.42	2.19	0.83	242.89
20160921	310.3	245.65	85.53	226.40	84.96	2.77	1.92	1.62	227.42
20161004	310.3	277.02	86.58	244.28	86.20	2.28	2.05	1.34	192.78
20161005	310.3	236.56	85.10	225.30	85.15	7.44	1.86	4.32	162.66
20161006.1	310.3	243.45	85.21	233.50	85.64	6.77	1.92	3.94	165.33
20161006.2	310.3	242.86	85.21	233.50	85.64	6.77	1.92	3.94	165.33
20161006.3	310.3	293.05	86.08	241.34	85.96	5.35	2.00	3.11	172.56
20161007	310.3	323.95	88.77	235.85	85.71	6.17	1.95	3.59	170.40
20161012	310.3	291.89	86.49	245.70	86.21	5.42	2.03	3.16	172.89

Table 2: Test Matrix, Initial, and Boundary Conditions

Date	TC96 (0.0%)	TC95 (0.7%)	TC94 (6.0%)	TC93 (15.5%)	TC92 (28.1%)	TC91 (42.5%)	TC90 (57.5%)	TC89 (71.9%)	TC75 (84.4%)	TC74 (94.0%)	TC73 (99.3%)	TC55 (Lid Middle)	TC60 (Lid Half-Way)	TC68 (Lid Edge)	NVF Duration	Tank Pressure at NVF End	Tank Temperature at NVF End	LL at NVF End
Test Name	K	K	K	K	K	K	K	K	K	K	K	K	K	K	seconds	kPa	K	% Fill
20160914	262.11	251.80	247.51	204.69	201.11	263.19	229.77	266.96	224.95	242.95	274.28	233.93	236.69	272.20	24	414.24	233.81	1.13
20160921	259.94	241.76	233.37	157.98	162.73	260.47	198.76	266.55	201.98	216.15	278.63	223.51	224.18	277.77	1735	320.35	109.32	89.68
20161004	94.59	91.39	142.84	156.65	172.09	203.68	196.15	184.30	189.26	196.65	226.92	236.94	239.70	272.13	33	395.70	174.56	2.34
20161005	90.82	90.81	89.38	103.44	131.18	168.82	163.98	148.92	150.68	157.27	195.56	222.56	222.79	275.70	1479	297.56	88.29	91.77
20161006.1	91.34	91.09	89.82	111.27	134.72	171.84	166.59	151.41	153.15	160.05	197.73	225.43	226.23	276.40	1622	303.17	88.46	94.05
20161006.2	91.34	91.09	89.82	111.27	134.72	171.84	166.59	151.41	153.15	160.05	197.73	225.43	226.23	276.40	1634	302.53	88.41	94.88
20161006.3	92.43	91.37	90.16	123.95	143.53	179.66	172.68	157.79	160.82	169.32	210.22	232.80	234.31	282.02	144	410.37	140.94	6.87
20161007	92.20	91.43	89.98	122.10	141.55	178.52	172.47	157.38	159.58	166.54	204.17	228.39	229.92	278.98	700	406.61	121.05	16.34
20161012	92.37	91.69	90.40	126.55	145.26	181.68	175.44	160.56	163.43	170.43	207.78	229.70	231.44	278.66	111	416.93	144.75	5.81

Table 3: Test Matrix, Initial, Boundary, and Final Conditions

A full explanation of the different parameters in Tables 2 and 3 can be found in [4]. For example, liquid level in the tank was calculated by dividing the volume of the liquid in the tank by the total tank volume at any point in time, ignoring the small volume change as the tank contracts with colder temperature, after some algebraic manipulation:

$$Liquid\ Level = \frac{V_{liquid}}{V_{tank}} = \frac{m_{liquid}}{\rho_{liquid} V_{tank}} = \frac{\left(m_{LC} - m_{CRYOTE}\right) - \rho_{vapor} V_{tank}}{\rho_{liquid} V_{tank} - \rho_{vapor} V_{tank}} \tag{3}$$

Similarly, "CRYOTE Mass Liquid at NVF Start" and "CRYOTE Mass Vapor at NVF Start" are calculated using conservation of mass and a volume constraint:

$$m_{LC} - m_{CRYOTE} = m_{liquid} + m_{vapor} \tag{4}$$

$$V_{tank} = V_{liquid} + V_{vapor} \tag{5}$$

where m_{CRYOTE} is the mass of the empty receiver tank. Substituting the known liquid and vapor densities using REFPROP [29], Equation 5 becomes:

$$V_{tank} = \frac{m_{liquid}}{\rho_{liquid}} + \frac{m_{vapor}}{\rho_{vapor}} \tag{6}$$

Using the known liquid level:

$$m_{liquid} = \rho_{liquid} V_{tank} LL \tag{7}$$

$$m_{vapor} = \rho_{vapor} V_{tank} \left(1 - LL\right) \tag{8}$$

Some additional points to consider: First, the temperature dependent specific heat of the 304SS lid and Ti6-4 tank walls were obtained from Marquardt et al. [30] and the Titanium Metals Corporation [31], respectively. The density, thermal conductivity, and specific heat as a function of temperature were imported into Thermal Desktop and applied to the solid finite element nodes that composed the solid wall and the lid of the model. Thermal Desktop uses an internal property file with values calculated from REFPROP Version 9.1 for the fluid properties of nitrogen [29]. Second, on account of a thin tank wall thickness, the measured external tank wall temperature can be used to approximate the internal wall temperature. Lastly, parasitic heat leak for this test series is quite small relative to the flow energy of the fluid and thus excluded from the Thermal Desktop model considerations.

For the purposes of this study the conditions at the start of NVF are important, as well as the conditions at the end of fill. The last column of Table 3 shows the liquid level (LL) or fill level at the end of NVF. It can be seen that many of the tests failed prematurely and did not reach a liquid level near or above 90% because the pressure in the tank exceeded the MEOP. Using this metric all tests can be classified as either “Successful” or “Failed.” Results will be presented separately for these two different test types. Note also that the test name corresponds to year, month, day (ex. 20160904 is September 9, 2016).

5.0 Description of the Model

Thermal Desktop is a multi-node, solid-fluid solver modeling tool that can provide relatively high-fidelity solutions without the high computational cost of higher order models such

as CFD. CAD models can be imported and meshed to create a network of finite elements to represent solid geometry [32]. TD interfaces with SpaceClaim where the CAD geometry designed in another program can be simplified and then meshed when imported into TD's AutoCAD interface. The user has a significant amount of control over the mesh creation (maximum number of nodes, allowable curvature, allowable scaling) both globally and at the local level for individual surfaces or solids. For the CRYOTE-2 Receiver Tank, the default values were used, because this is a relatively simple spherical geometry without small features or sharp edges. The resulting mesh contained 530 solid nodes.

SINDA/FLUINT is the thermal/fluid solution engine used within Thermal Desktop. SINDA solves the conduction and thermal capacitance of the thermal network in the model in addition to outside heat loads or radiation [32]. Within SINDA, the network consists of nodes and conductors. Energy is stored in the nodes and transferred via the conductors between nodes to create the network. FLUINT solves the thermohydraulic network in the model, both fluid flow through a network or accumulation in a tank [32]. The two solvers work simultaneous to converge on a solution. Within FLUINT, the fluid network consists of fluid lumps and fluid paths. In this model, two types of fluid lumps were used: tanks and plena. A tank is a lump representing a finite control volume governed by differential equations of mass conversation and energy conservation. In contrast a plenum is a lump with an infinite volume and represents a boundary condition, in this case the inlet flow conditions into the receiver tank. Fluid paths are governed by differential equations for momentum conservation and connect two fluid lumps. Heat transfer between the fluid lumps and solid nodes is governed by a tie.

Only the CRYOTE-2 receiver tank was constructed in this Thermal Desktop model. The tank wall and lid were modeled using finite elements with the material properties of stainless

steel (SS304) and Ti applied. The fluid inside the tank is represented using twin lumps, with a single lump representing the vapor and liquid phases that are at the same pressure but different temperatures. The quality of each lump is also tracked independently, meaning that the "vapor" and "liquid" lump can either contain subcooled liquid, saturated liquid, two-phase fluid, saturated vapor, or superheated vapor. Three different paths represent the inlet flow into the tank, each representing one of the three nozzle injectors.

5.1 Compartments and Bays

Previous work on modeling tank chilldown has focused on a simple dip tube or bottom-fill injector. A compartment is used to represent the location of the internal volume that is occupied by the fluid. The volume of the compartment does not change with time and is occupied by twin lumps so that the volume of the two lumps combined at any point in time is always equal to the internal volume of the tank. The compartment will also track the location of the liquid-vapor interface as the tank drains or fills over time. In these models, a single inlet flow path is directed to the bottom of the tank to represent a bottom-fill scenario. As liquid begins to accumulate in the bottom of the tank during a fill, the flow is directed into the liquid lump first and only enters the vapor lump through evaporation across the liquid-vapor interface. All mass transfer across the interface is tracked by a separate flow path in TD.

Due to the different injection patterns of the 2016 injector from Figure 3, the tank wall was sprayed unevenly and therefore chilled down at the different rates. This resulted in variation in wall temperature at different tank wall heights at the start of fill. For example, as shown in Figure 4 for Test 20160921, most of the flow was directed at the level of TC92 and TC93, and these regions are significantly colder than the surrounding areas at the start of NVF. To represent these different cooling rates, the compartment in the tank was split into various bays based on the

height of the respective thermocouple. With these different sections, the inlet flow path can be split between the different tank heights to represent where more fluid is directly in contact with the wall. This effectively separated the tank horizontally into different bays with fluid being able to freely pass between them without a separate interface. The distribution of the flow for the three different injector types is shown in Table 4.

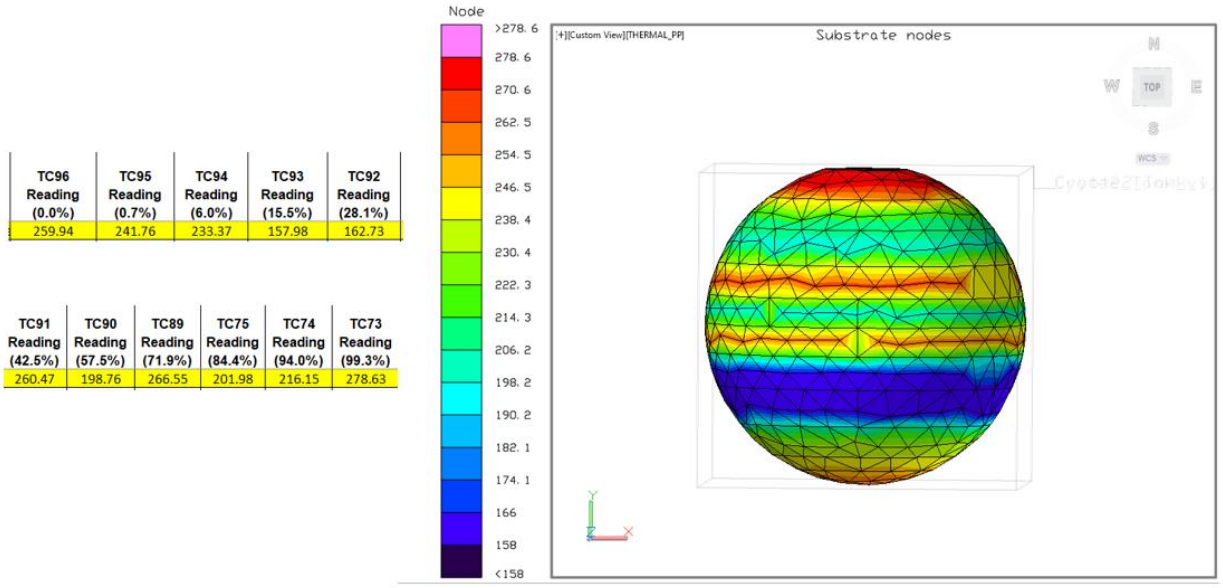

Figure 4: Thermal Desktop Model at the Start of No-Vent Fill for Test 20160921

5.2 Inlet Flow Rate Control

Because of the lack of inlet flow rate data, two different methods were used to model each test case. The first, hereafter referred to as "Mass Controlled," fed the flow rate data backed out from the load cells directly into the model as an input. This was the first method used but resulted in overprediction of the initial pressure spike inside the receiver tank likely attributed to a possible overprediction of wall boiling or an underprediction of condensation. In order to attempt to combat this issue, the second method was developed. This second method, hereafter

referred to as “Pressure Controlled,” used the pressure difference between the inlet pressure and tank pressure with the known coefficient of discharge to determine a flow rate using Equation 1. Both of these methods result in different flow rates and therefore different pressure curves and fill levels. Results for these two methods will be discussed subsequently.

Thermocouple Location	3-spray nozzle
TC73-89	33.3%
TC90-93	55.5%
TC94-96	11.2%

Table 4: Flow Distribution at Different Tank Heights for 2016 Tests

5.3 Wall Temperatures

The original test dataset used a mass-averaged temperature reading to represent the overall wall outside wall temperature. However, the Thermal Desktop model calculates average wall temperature by using the arithmetic average of all finite element nodes in the model, meaning all nodes were summed (weighted equally) and divided by the total number of nodes to get the average. Because all nodes are weighted equally, this arithmetic average gives a different result than the mass-averaged temperature from the data. Even though there is generally good agreement between these two metrics, the difference in methodology may explain some of the error.

6.0 Results and Discussion

6.1 Successful Tests

Figure 5 plots Thermal Desktop model results for Test 20160921, a successful NVF at an average starting wall temperature of 227K. Figures 5a-c plot results for tank pressure, fill level, and average wall temperature for the mass- controlled method and Figures 5d-f plot those

variables for the Pressure Controlled method. The data shows the classic stages of NVF described in [4], an initial pressure rise due to flash evaporation at the inlet and boiling at the wall as the tank wall moves through the various transition points on the quenching boiling curve. Soon after, the pressure exhibits the roll-over as condensation at the liquid-vapor (L/V) interface overtakes boiling at the wall. The tank fills with liquid. The final stage is the "piston-cylinder" stage where the ullage compresses, causing the receiver tank pressure to equilibrate with the supply pressure. At this point, the receiver tank is >90% full. Figure 5b shows a near linear increase in receiver tank fill level during NVF as liquid rapidly accumulates. Close inspection shows a slightly steeper accumulation during the remainder of chilldown after the start of NVF for the first ~300s followed by a final steeper accumulation during the final portion of transfer. Meanwhile the average wall temperature in Figure 5c, dominated by film boiling, gradually pass through film then transition then nucleate boiling before bottoming out.

Figure 5a shows that Mass Controlled Thermal Desktop model predicts the initial pressure rise well but then over-predicts the pressure spike likely attributed to overprediction of boiling at the wall or underprediction of condensation as mentioned previously. The model-predicted pressure then sharply decreases and then remains fairly flat for the remainder of the test. The final predicted pressure is ~33% higher than the data, despite predicting a successful fill. Figure 5b shows the predicted fill level agrees well with the data despite deviation in the predicted pressure; the slope change is captured well. Meanwhile, Figure 5c shows that the wall chilldown rate is under-predicted relative to the data because of the leveling off in flow rate

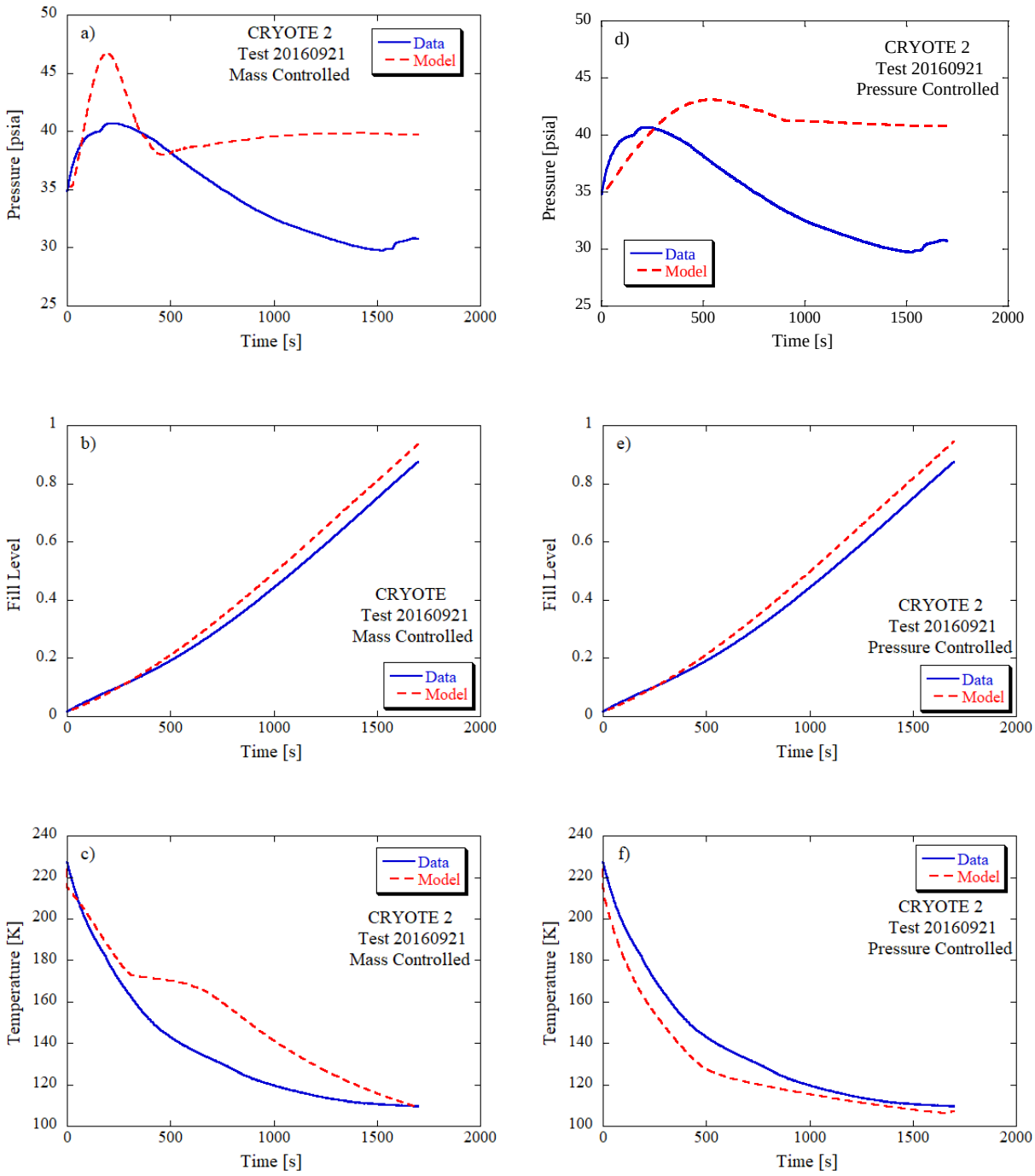

Figure 5: Test 20160921: a) Mass Controlled Pressure Rise, b) Mass Controlled Fill Level, c) Mass Controlled Average Temperature, d) Pressure Controlled Pressure Rise, e) Pressure Controlled Fill Level, and f) Pressure Controlled Average Temperature

For the Pressure Controlled model in Figure 5d, Thermal Desktop again over-predicts the pressure spike, but here, the peak is shifted to later in the test relative to Figure 5a. The final pressure is again over-predicted by ~33%. Figure 5e shows the fill level is again slightly overpredicted and Figure 5f shows the predicted wall chilldown rate is faster than the data. The wall cools down faster for the Pressure Controlled model due to the higher flow rate at the beginning of the simulation relative to the Mass Controlled. Overall, Thermal Desktop does a reasonably good job at predicting fill level and wall temperature but struggles to predict the pressure for this high delta-T NVF successful fill case.

Figure 6 plots Thermal Desktop model predictions against the data for Test 20161006.1, a successful NVF at a starting wall temperature of 165K. For Mass Controlled, the model predicted pressure is again overpredicted and the pressure remains high for the duration of the test, likely attributed to either overprediction of boiling at the wall or underprediction of condensation at the wall;; the final pressure is off by ~40%. Fill level is again slightly overpredicted but this time wall temperature cooling rate is overpredicted. Figures 6d-f show slightly better prediction for the Pressure Controlled case; here the pressure spike and rollover are predicted in the model, and the final pressure is only ~17% off from the data. The overprediction in fill level is slightly worse for Pressure Controlled over Mass Controlled case. Because the Pressure Controlled case's flow rate is driven by the pressure differential between the inlet and receiver tank, flow rate fluctuates significantly over the course of the test. Particularly when the pressure difference is greatest near the start of the test, the flow rate increases and there is a spike in the fill level. As the pressure evens out, the flow rate and resultant fill level also taper off. This early increase in fill level also results in a faster chilldown

of the nodes at the bottom of the tank and faster decrease in average tank wall temperature as compared to the Mass Controlled model.

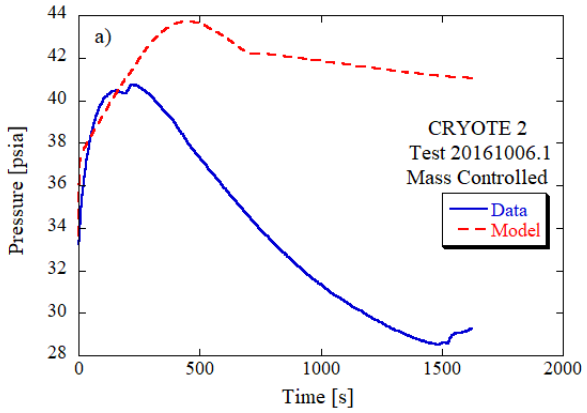

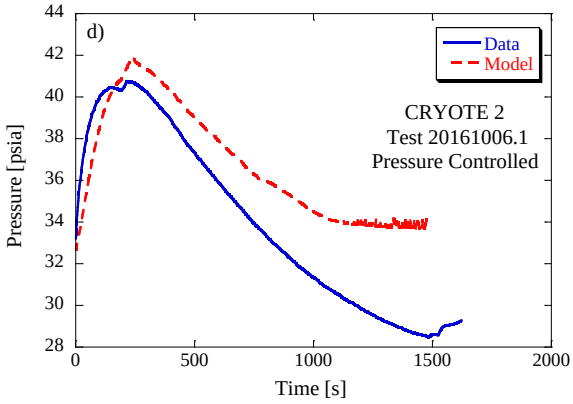

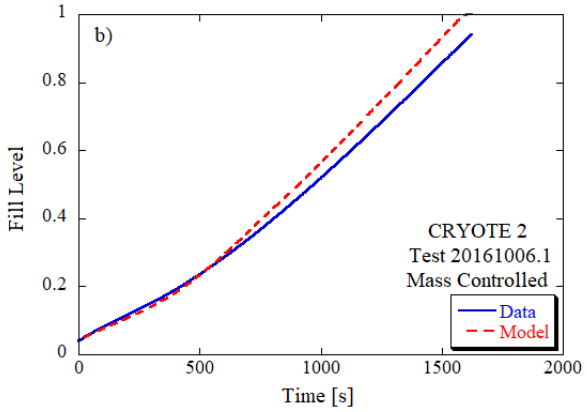

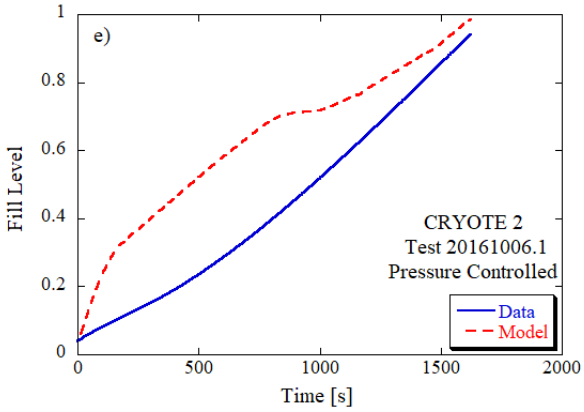

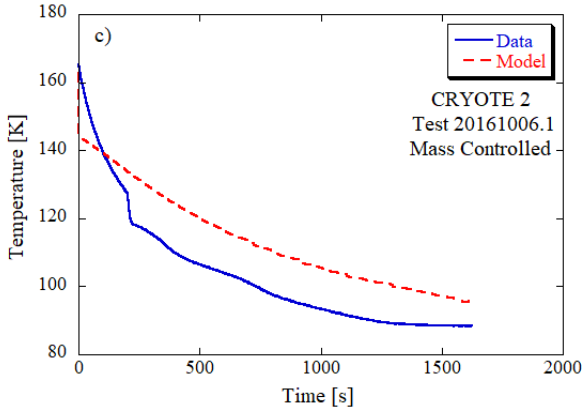

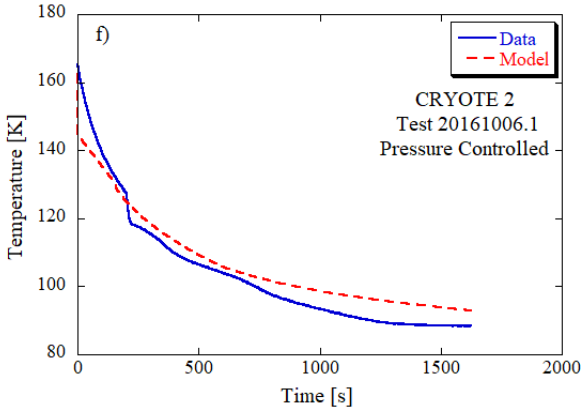

Figure 6: Test 20161006.1: a) Mass Controlled Pressure Rise, b) Mass Controlled Fill Level, c) Mass Controlled Average Temperature, d) Pressure Controlled Pressure Rise, e) Pressure Controlled Fill Level, and f) Pressure Controlled Average Temperature

6.2 Unsuccessful Tests

Figure 7 plots Thermal Desktop model predictions against the data for Test 20161004, an unsuccessful fill at an initial wall temperature of 193K. Figure 7a shows the model tracks the pressure rise rate and stall with good accuracy. Figure 5b shows the Mass Controlled method drastically underpredicts the fill level throughout the test, and Figure 5c shows the model predicted chilldown rate is overpredicted initially for the first 100s, but then underpredicts the chilldown slightly for the remainder of the failed fill. For Pressure Controlled, Figure 7d shows the opposite trend; the pressure rise rate is underpredicted, but then agrees well with the data after the first 200s. Figure 7e shows the model underpredicts the fill level again, but not as drastically as in the Mass Controlled method. Finally, Figure 7f shows similar behavior as Figure 7c, but the underprediction of wall chilldown rate is higher for Pressure Controlled scheme.

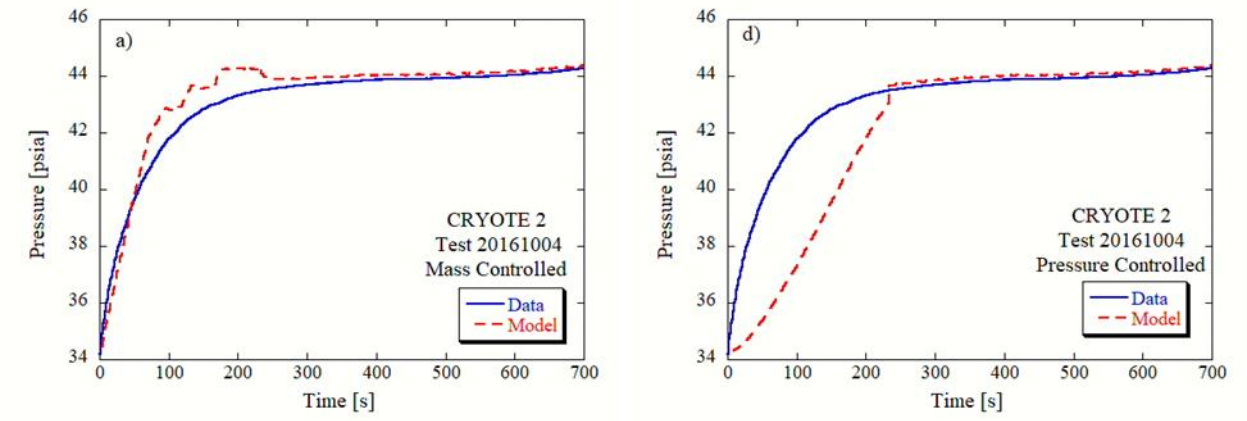

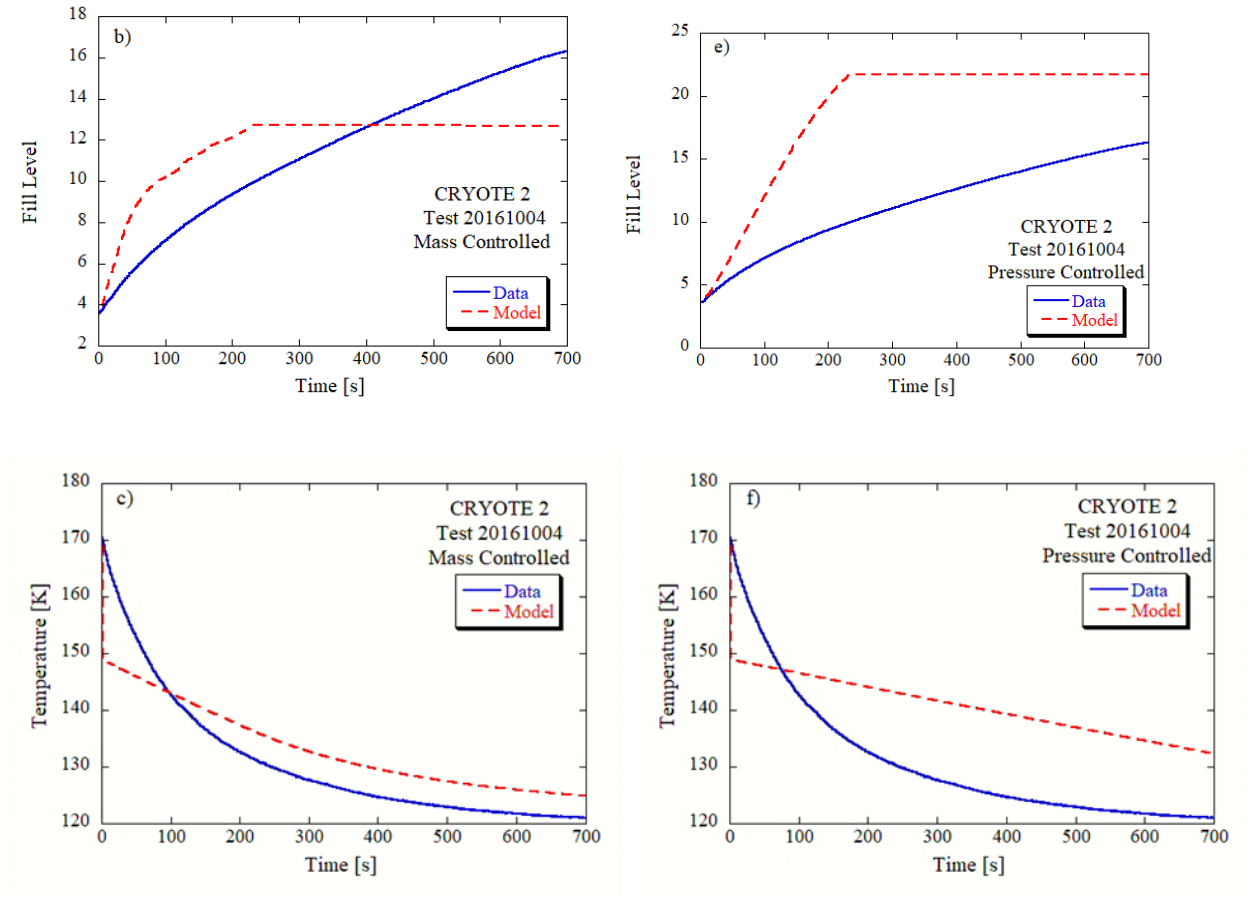

Figure 7: Test 20161004: a) Mass Controlled Pressure Rise, b) Mass Controlled Fill Level, c) Mass Controlled Average Temperature, d) Pressure Controlled Pressure Rise, e) Pressure Controlled Fill Level, and f) Pressure Controlled Average Temperature

Figure 8 shows model predictions for Test 20161012 at a starting wall temperature of 173K. This test lasted less than a minute, and over that time both schemes show that the model predicts the pressure rise rate and change in fill level well. The main discrepancy between data and model is in the predicted wall temperature; both schemes overpredict the wall chilldown rate, but then there is a crossover and eventual underprediction. Overall, Pressure Controlled scheme performs better than the Mass Controlled scheme.

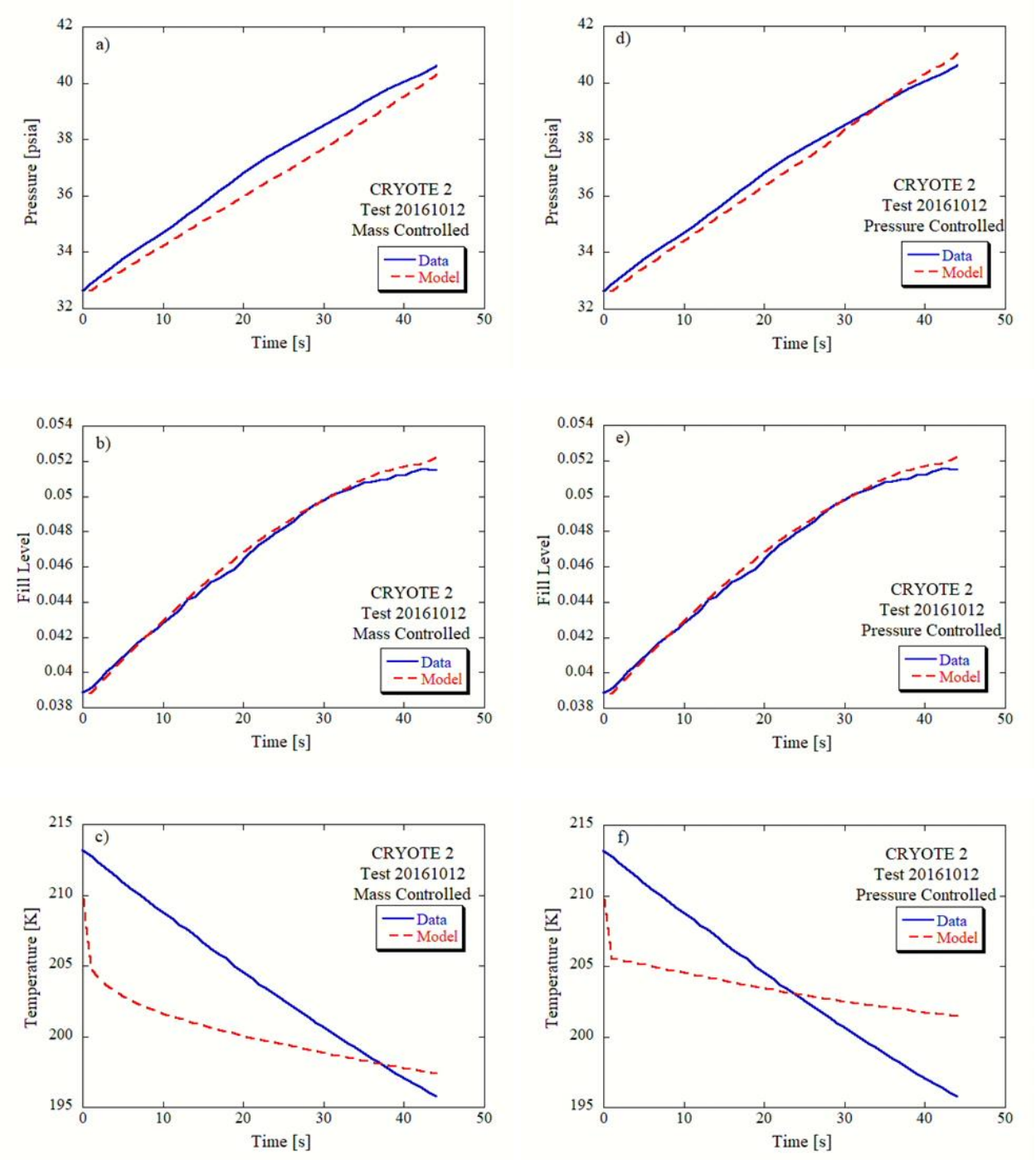

Figure 8: Test 20161012: a) Mass Controlled Pressure Rise, b) Mass Controlled Fill Level, c) Mass Controlled Average Temperature, d) Pressure Controlled Pressure Rise, e) Pressure Controlled Fill Level, and f) Pressure Controlled Average Temperature

6.3 Consolidated Results and General Discussion

To quantify error between data and model, a mean absolute error (MAE) value is computed for pressure, fill level, and wall temperature data point time step and summed using Equation 9:

$$\text{MAE}=\frac{1}{N}\sum\frac{|\text{data-model}|}{\text{data}} \tag{9}$$

To convert to a mean absolute percentage error (MAPE), the MAE value was multiplied by 100. MAPE results are shown in Table 5. Overall, pressure is predicted within 29% for all cases and average wall temperature within 20% of the data for all 8 cases. Error is as high as 79% for fill level.

There were several very apparent differences between the Mass and Pressure Controlled results. The fill level from the model always matched within 5% from the data for the Mass Controlled method for all cases. This agreement is expected because the load cell data is fed directly into the model as an input. Any discrepancy between the two numbers is likely due to slightly different physics e.g., more or less evaporation in the tank resulting in a lower or higher mass. However, for the Pressure Controlled cases there were significantly higher MAPEs for the fill level. This large discrepancy is due to the difference in inlet flow rate between the two methods. However, for several cases the final fill level, and therefore the total mass injected into the tank, was very similar to the Mass Controlled result.

Conversely, the opposite trend holds for comparing the pressure rise in the tank between the two modeling methods although the trend is not as significant as the difference in fill levels. The Mass Controlled method often resulted in lower MAPEs for the pressure than the Pressure Controlled method. Again, this difference can be attributed to the different flow rates. The

Pressure Controlled method is directly tied to the reported pressure in the receiver tank, and therefore gives better agreement with the test data.

Test	Success or Fail?	Pressure MAPE (%)	Fill Level MAPE (%)	Average Wall Temperature MAPE (%)
20160921	S	17.1	9.6	12.1
20161005	S	19.2	2.4	20.1
20161006.1	S	25.0	7.0	11.0
20161006.2	S	25.0	7.0	11.0
20161004	F	0.9	5.6	3.7
20161006.3	F	3.3	1.8	2.0
20161007	F	27.8	1.6	6.6
20161012	F	1.6	0.5	1.9

Table 5: Resultant Mean Absolute Percentage Error for Pressure, Fill Level, and Average Tank Wall Temperature using Mass Controlled Modeling Approach

There were also notable differences between the successful and failed tests. In looking at the fill level and average temperatures, the failed tests often had lower MAPEs than the successful tests. This is largely due to the decreased time of the failed tests, most of which were under two minutes in length. For such a short duration, the fill level and average wall temperature do not have time to vary significantly and so result in very small MAPEs. However,

for the pressure rise inside the tank there is not a significant difference between the successful and failed tests.

Test	Success or Fail?	Pressure MAPE (%)	Fill Level MAPE (%)	Average Wall Temperature MAPE (%)
20160921	S	21.2	10.4	5.9
20161005	S	10.5	60.8	9.6
20161006.1	S	16.3	78.7	4.6
20161006.2	S	8.3	78.7	4.6
20161004	F	2.7	4.6	9.2
20161006.3	F	2.8	1.8	2.0
20161007	F	28.7	1.6	12.3
20161012	F	21.2	10.4	5.9

Table 6: Resultant Mean Absolute Percentage Error for Pressure, Fill Level, and Average Tank Wall Temperature using Pressure Controlled Modeling Approach

7.0 Conclusion

This paper presented validation of a Thermal Desktop model against the 2016 CRYOTE-2 liquid nitrogen tank transfer experiments. This test series represents the most difficult model validation case performed for Thermal Desktop to-date, due to the rapid transients and high delta-T flow physics and heat transfer. Two modeling schemes were presented, one that controlled the mass flow rate as the boundary condition, and one that relied on inlet pressure as

the boundary condition. Both schemes do a reasonable job at predicting pressure within 29% and wall temperature within 21% of the data across the 8 test cases examined. the largest disparity between the two methods is in predicting fill level, which is off by as much as 79% of the da. Nonetheless, Thermal Desktop does a very reasonable job at predicting performance for this difficult validation case and such high initial wall temperature NVFs and will continue to be a useful tool for predicting various cryogenic fluid management phenomena.

Acknowledgements

This work was funded by the Reduced Gravity Cryogenic Transfer Project under the Cryogenic Fluid Management Project under the Space Technology Mission Directorate at NASA.

[1] Chato, D.J., and Sanabria, R. "Review and Test of Chilldown Methods for Space-Based Cryogenic Tanks" NASA-TM-104458 June, 1991.

[2] Keefer, K.A. and Hartwig, J.W. "Development and Validation of an Analytical Charge-Hold-Vent Model for Cryogenic Tank Chilldown" International Journal of Heat and Mass Transfer 101, 175 – 189. 2016.

[3] Kartuzova, O. and Kassemi, M. "Modeling K-Site LH_2 Tank Chilldown and No Vent Fill in Normal Gravity" *AIAA-2017-4662, 53rd AIAA Joint Propulsion Conference,* Atlanta, GA, July 10 – 12, 2017.

[4] Hartwig, J.W., Rhys, N., Clark, J., Mercado, M., LeClair, A., and Majumdar, A. "Test Data Analysis of the Vented Chill, No-Vent Fill Liquid Nitrogen CRYOTE-2 Experiments" *International Journal of Heat and Mass Transfer* 167, 120781. 2021.

[5] Hartwig, J.W., Mercado, M., and Moore, R. “Test Data Analysis of the Liquid Hydrogen Chilldown and Fill Transfer Experiments of a Flightweight Aluminum Tank” *International Journal of Heat and Mass Transfer* 202, 123766. 2023a.

[6] Hartwig, J.W., Stevens, J., Rhys, N. Clark, J., LeClair, A., and Majumdar, A. “Test Data Analysis of the CRYOTE-2 TVS Augmented Top Spray Injector Liquid Nitrogen Transfer Experiments” *International Journal of Heat and Mass Transfer* 194, 122986. 2022.

[7] Fester, D.A. and Page, G.R. “Liquid Fluorine No-Vent Loading Studies” AIAA-69-579 5th Joint Propulsion Conference, Colorado, CO, June 9 – 13, 1969.

[8] Chato, D.J., Moran, M.E., and Nyland, T.W. “Initial Experimentation on the Nonvented Fill of a 0.14 m^3 (5 ft^3) Dewar with Nitrogen and Hydrogen” NASA-TM-103155 June, 1990.

[9] Moran, M.E., Nyland, T.W., and Papell, S.S. “Liquid Transfer Cryogenic Test Facility – Initial Hydrogen and Nitrogen No-Vent Fill Data” NASA-TM-102572 March, 1990.

[10] Moran, M.E., Nyland, T.W., and Driscoll, S.L. “Hydrogen No-Vent Fill Testing in a 1.2 Cubic Foot (34 Liter) Tank” NASA-TM-105273 October, 1991.

[11] Chato, D.J. “Ground Testing on the Nonvented Fill Method of Orbital Propellant Transfer: Results of Initial Test Series” NASA-TM-91-2326 June, 1991.

[12] Moran, M.E. and Nyland, T.W. “Hydrogen No-Vent Fill Testing in a 5 Cubic Foot (142 Liter) Tank using Spray Nozzle and Spray Bar Liquid Injection” NASA-TM-105759 July, 1992.

[13] Chato, D.J. “Ground Testing for the No-Vent Fill of Cryogenic Tanks: Results of Tests for a 71 Cubic Foot Tank” NASA-TM-106293 June, 1993.

[14] Wang, C. and Wang, R. “The Effects of Vertical and Horizontal Placement on No-Vent Fill of Cryogenic Insulated Vessels” Cryogenics 50, 480 – 485. 2010.

[15] Wang, C., Li, Y., and Wang, R. “Performance Comparison between No-Vent and Vented Fills in Vertical Thermal-Insulated Cryogenic Cylinders” Experimental Thermal and Fluid Sciences 35, 311 – 318. 2011.

[16] Kim, Y., Lee, C., Park, J., Seo, M., and Jeong, S. “Experimental Investigation on No-Vent Fill Process using Tetrafluoromethane (CF4)” Cryogenics 74, 123 – 130. 2016.

[17] Flachbart, R.H., Hedayat, A., Holt, K., Sims, J., Johnson, E.F., Hastings, L.J., and Lak, T. “Large-Scale Liquid Hydrogen Tank Rapid Chill and Fill Testing for the Advanced Shuttle Upper Stage Concept” *NASA-TP-2013-217482,* April, 2013.

[18] Ganesan, V., Patel, R., Hartwig, J.W., and Mudawar, I. “Universal Critical Heat Flux (CHF) Correlations for Cryogenic Flow Boiling in Uniformly Heated Tubes” *International Journal of Heat and Mass Transfer* 166, 120678. 2021.

[19] Ganesan, V., Patel, R., Hartwig, J.W., and Mudawar, I. “Review of Databases and Correlations for Saturated Flow Boiling Heat Transfer Coefficient for Cryogens in Uniformly Heated Tubes, and Development of New Consolidated Database and Universal Correlations” *International Journal of Heat and Mass Transfer* 179. 121656. 2021.

[20] Ganesan, V., Patel, R., Hartwig, J.W., and Mudawar, I. “Universal Correlations for Post-CHF Saturated and Superheated Flow Film Boiling Heat Transfer Coefficient, Minimum Heat Flux and Rewet Temperature for Cryogenic Fluids in Uniformly Heated Tubes” *International Journal of Heat and Mass Transfer* 195, 123054. 2022.

[21] Clark, J. and Hartwig, J.W. “Assessment of Prediction and Efficiency Parameters for Cryogenic No-Vent Fill” *Cryogenics* 117, 103309. 2021.

[22] Majumdar, A., LeClair, A., Martin, A., Rhys, N., and Hartwig, J.W. “Numerical Modeling of No Vent Fill of a Cryogenic Tank” *AIAA-2020-3797, 2020 Joint Propulsion Conference* New Orleans, LA, August 24 – 26, 2020.

[23] Majumdar, A., LeClair, A., Hartwig, J.W., and Ghiaasiaan, M. “Numerical Modeling of No Vent Filling of a Cryogenic Tank with Thermodynamic Vent System Augmented Injector” *Cryogenics* 2022.

[24] Majumdar, A., LeClair, A., Hartwig, J.W., and Ghiaasiaan, M. “Numerical Modeling of No Vent Filling of a Cryogenic Tank with Thermodynamic Vent System Augmented Injector” *Cryogenics* 131, 103651. 2023.

[25] White, D. “FLUENT Conjugate Heat Transfer Simulations of K-Site LH_2 Tank Chilldown” *RGCT-DOC-FY20-03*, June 19, 2020.

[26] Hartwig, J.W., Esser, N., Jain, S., Souders, D., Tafuni, A., and Prasad-Varghese, A. “CFD Modeling of a Bi-Directional Propellant Management Device inside a Cryogenic Propellant Tank Onboard a Parabolic Flight” *Journal of Spacecraft and Rockets* 2023b.

[27] Gravlee, M., Kutter, B., Wollen, M., Rhys, N.O., and Walls, L.K. Nyland, T.W. “CRYOTE (Cryogenic Orbital Testbed) Concept” AIAA-09-6440 September, 2009.

[28] BETE. (2019). “TF Full Cone” Retrieved October 31, 2019, from https://www.bete.com/PDFs/BETE_TF.pdf

[29] Lemmon, E.W., Bell, I.H., Huber, M.L., McLinden, M.O. “NIST Standard Reference Database 23: Reference Fluid Thermodynamic and Transport Properties-REFPROP,

Version 9.0" National Institute of Standards and Technology, Standard Reference Data Program, Gaithersburg, 2010.

[30] Marquardt, E.D., Le, J.P., and Radebaugh, R. "Cryogenic Material Properties Database" 11th International Cryocooler Conference June, 2000.

[31] Titanium Metals Corporation. (1998). "Properties and Processing of TIMETAL 6-4" Retrieved October 31, 2019, from https://www.timet.com/assets/local/documents/technicalmanuals /TIMETAL_6-4_Properties.pdf.

[32] C&R Technologies. TD Suite Manual For Thermal Desktop, TD Direct, and SINDA/FLUINT. Version 6.3, Thermal Desktop Patch 13, SINDA/FLUINT Patch 10, 2022.